J Mol Model (2013) 19:2197–2203
DOI 10.1007/s00894-012-1751-2

ORIGINAL PAPER

Sensing behavior of Al-rich AlN nanotube toward hydrogen cyanide

Javad Beheshtian · Ali Ahmadi Peyghan · Zargham Bagheri

Received: 16 September 2012 / Accepted: 29 December 2012 / Published online: 26 January 2013

Abstract In order to explore a sensor for detection of toxic hydrogen cyanide (HCN) molecules, interaction of pristine and defected Al-rich aluminum nitride nanotubes (AlNNT) with a HCN molecule has been investigated using density functional theory calculations in terms of energetic, geometric, and electronic properties. It has been found that unlike the pristine AlNNT, the Al-rich AlNNT can effectively interact with the HCN molecule so that its conductivity changes upon the exposure to this molecule. The adsorption energies of HCN on the pristine and defected AlNNTs have been calculated to be in the range of −0.16 to −0.62 eV and −1.75 to −2.21 eV, respectively. We believe that creating Al-rich defects may be a good strategy for improving the sensitivity of these tubes toward HCN molecules, which cannot be trapped and detected by the pristine AlNNT.

Keywords B3LYP · DFT · Nanotube · Sensor · Theoretical study

Introduction

Gas adsorption on the nanotubes is of great importance and interest in both essential research and application of nanotubes. The adsorptive characteristics of nanotubes in gas phase have resulted in their use in gas sensors, storage of fuels, and removal of hazardous pollutants from gas streams [1–3]. So far, many different aspects of nanotube/adsorbates have been experimentally explored [4–6]. Moreover, different kinds of nanotubes such as carbon nanotubes (CNTs), boron nitride nanotubes (BNNTs), silicon carbide nanotubes, zinc oxide nanotubes, and TiO_2 nanotubes have been theoretically investigated for gas molecule adsorption [7–20]. Meanwhile, the efficiency of gas adsorption on the nanotubes can be enhanced by creating topological defects [21] or doping [22].

In recent years, III–V semiconductor nanostructures (nanotubes, nanowires, nanoclusters, and nanotips) have attracted enhanced scientific interest due to their numerous technological applications in nanoengineering. Among the group III nitrides, AlN is the semiconductor with the largest bandgap, which is known for having high temperature stability, considerable thermal conductivity, low thermal expansion, resistance toward chemicals and gases used in semiconductor processing, and reliable dielectric properties [23, 24]. Zhang et al. have predicted that AlNNTs are energetically favorable and arrange in a hexagonal network adopting sp^2 hybridization for both N and Al atoms [25]. Tondare et al. have successfully synthesized the AlNNTs with diameter ranging from 30 to 80 nm [26]. Recently, some other reports have been published on the synthesis of AlNNTs through different methods [27, 28]. The electronic properties of the AlNNTs are different from that of the CNTs. It is already well known that CNTs can be either metallic or semiconducting, depending on their chirality and radius [29], whereas AlNNTs are semiconductors with wide energy bandgaps almost regardless of the diameter, chirality, and the number of the walls [30].

The environmental gas monitoring is considered as an important issue and much research has been focused on development of suitable gas-sensitive materials for

J. Beheshtian
Department of Chemistry, Shahid Rajaee Teacher Training University, P.O. Box: 16875-163, Tehran, Iran

A. A. Peyghan (✉)
Young Researchers Club, Islamic Azad University, Islamshahr Branch,
Tehran, Iran
e-mail: ahmadi.iau@gmail.com

Z. Bagheri
Physics group, Science Department, Islamic Azad University, Islamshahr Branch, P.O. Box: 33135-369, Islamshahr, Tehran, Iran

continuous monitoring and setting off alarms for hazardous chemical vapors beyond the specified level. Hydrogen cyanide (HCN) is highly lethal to man and animals, so the monitoring and control of its exposure in both industrial and residential environments are of special interest. Therefore, effective methods for monitoring and suppressing the HCN concentration have been highly demanded for atmospheric environmental measurements and controls [31]. Recently, Zhang et al. have theoretically shown that silicon-doped BNNTs would be potential candidates for HCN molecule detection [31]. In the present work, the interaction of HCN molecule with AlNNTs will be theoretically investigated based on analysis of structure, energies, electronic properties, etc. To this end, within the density functional theory (DFT) framework [32], we have tried to find the answers to the following questions: (1) whether there is a potential possibility of AlNNTs serving as a chemical sensor for HCN or not; (2) if not, what strategy can be applied to improve the sensitivity of AlNNTs toward toxic HCN?

Computational methods

A zigzag single-walled (5, 0) AlNNT consisting of 30 aluminum and 30 nitrogen atoms was considered in such a way that its end atoms were saturated with hydrogen atoms to avoid the boundary effects. The full geometry optimizations and property calculations were performed on the pristine and defected AlNNTs in the presence and absence of a HCN molecule using three-parameter hybrid generalized gradient approximation with the B3LYP functional and the 6–31G basis set including the d-polarization function (denoted as 6–31G(d)) as implemented in the GAMESS suite program [33]. Harmonic vibrational frequencies have also been calculated at the same level of theory, enabling us to confirm real minima. The B3LYP density functional has been previously shown to reproduce experimental properties and has been commonly used for nanotube structures [34–36]. It has also been demonstrated that the B3LYP provides an efficient and robust basis for calculations of III–V semiconductors by Tomic et al. [37], capable of reliably predicting both the ground state energies and the electronic structure. Length and diameter of the optimized pristine AlNNT were computed to be about 14.00 and 5.33 Å, respectively. The spin unrestricted calculations for defected AlNNT systems were performed in the presence and absence of a HCN molecule. The adsorption energy (E_{ad}) of a HCN molecule on the AlNNT is obtained using the following equation:

$$E_{ad} = E(\text{AlNNT/HCN}) - E(\text{AlNNT}) - E(\text{HCN}) + E_{BSSE}, \quad (1)$$

Table 1 Calculated adsorption and BSSE energies of HCN on the AlNNT (E_{ad}), HOMO energies (E_{HOMO}), LUMO energies (E_{LUMO}), and HOMO-LUMO energy gap (E_g) for the studied systems (Fig. 2). Energies are in eV

System	E_{ad}	E_{BSSE}	[a]Q_T (e)	E_{HOMO}	E_{LUMO}	E_g	[b]ΔE_g(%)
AlNNT	–	–	–	−6.31	−2.22	4.09	–
A	−0.16	0.07	0.002	−6.37	−2.31	4.06	0.7
B	−0.62	0.16	0.188	−6.31	−1.98	4.06	0.7

[a] Q is defined as the average of total Mulliken charge on the molecule

[b] The change of HOMO-LUMO gap of AlNNT after adsorption

where E (AlNNT/HCN) is the energy of the AlNNT/HCN complex, and E (HCN) and E (AlNNT) refer to the energy of an isolated HCN molecule and the pristine AlNNT, respectively. E_{BSSE} is the basis set superposition error (BSSE) corrected for all of the interaction energies (Tables 1 and 2) [38]. The negative value of E_{ad} indicates the exothermic character of the adsorption. GaussSum program [39] has been used to obtain DOS results.

Results and discussion

The optimized structure and density of state (DOS) plot of the AlNNT are shown in Fig. 1, in which two types of Al-N bonds can be identified; one with the length of 1.81 Å and in parallel with the tube axis, and another with the bond length of 1.82 Å, but not in parallel with the tube axis. The charge analysis using the Mulliken method indicates that about 0.27 *e* is transferred from the Al atom to its adjacent nitrogen atoms within the sidewall, indicating partially ionic character of the Al-N bonds in the sidewall. As shown by the calculated DOS and the energy gaps (E_g) between the highest occupied molecular orbitals (HOMOs) and the lowest unoccupied molecular orbitals (LUMOs) in Fig. 1 and

Table 2 Calculated adsorption BSSE energies of HCN on the Al-rich AlNNT (E_{ad}), HOMO energies (E_{HOMO}), LUMO energies (E_{LUMO}), and HOMO-LUMO energy gap (E_g) for HCN/Al-rich AlNNT systems (Fig. 4). Energies are in eV

System	E_{ad}	E_{BSSE}	[a]Q_T (e)	E_{HOMO}	E_{LUMO}	E_g	[b]ΔE_g(%)
Al-rich AlNNT	–	–	–	−5.37	−3.13	2.24	–
P	−2.12	0.21	−0.265	−5.19	−2.17	3.02	34.8
Q	−1.75	0.23	−0.310	−5.42	−2.39	3.03	35.2
R	−1.78	0.21	−0.327	−5.40	−2.51	2.88	28.5
S	−2.21	0.20	−0.313	−5.2	−2.20	3.00	33.9

[a] Q is defined as the average of total Mulliken charge on the molecule

[b] The change of HOMO-LUMO gap of defected AlNNT after adsorption

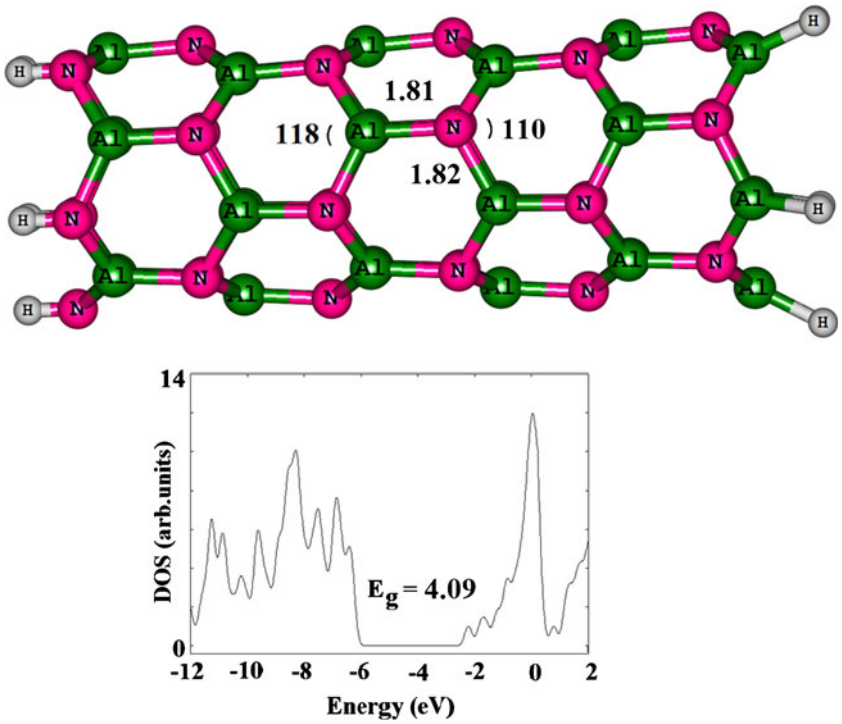

Fig. 1 Partial structure of AlNNT and its density of state (DOS). Distances are in Å

Table 1, the pristine AlNNT is found to be a semiconductor with a wide band gap of 4.09 eV.

HCN adsorption on the pristine AlNNT

In order to obtain the most stable configuration of a single-HCN-adsorbed on the AlNNT various possible initial adsorption geometries including single (hydrogen, carbon, or nitrogen), double (H–C or C–N) and triple H–C–N bonded atoms to Al and N atoms on different adsorption sites have been considered. However, only two local minima structures were obtained upon the relaxation processes (Fig. 2). More detailed information from simulation of different HCN-AlNNT systems including values of E_{ad}, E_g, and charge transfer (Q_T) of these configurations have been listed in Table 1. The configuration **A** stands for the hydrogen bonding between the hydrogen atom of the HCN molecule and the N atom of the nanotube with distance of 2.40 Å. In this configuration, a net charge of about 0.002 electron transfers from the molecule to the tube and its corresponding calculated E_{ads} value (Table 1) is about −0.16 eV. The small E_{ad} and transferred charge in this structure reveal the physical nature of the interaction. Calculated DOS plot (Fig. 2a) shows that the HCN adsorption through this configuration has no sensible effects on the electronic properties of AlNNT so that the E_g of the tube has slightly decreased from 4.09 to 4.06 eV.

As shown in Fig. 2b, the most stable configuration of the HCN/AlNNT system (**B**) is that in which the N atom of the HCN is close to an Al atom of the tube surface with equilibrium distance of 2.08 Å with the corresponding E_{ad} of −0.62 eV. It should be noted here that the stretching mode of C≡N bond in the adsorbed HCN occurs at slightly lower frequency (2098 cm^{-1}) in comparing with that in the free molecule (2214 cm^{-1}), confirming weakness of the interaction. However, more stability of this configuration in comparison with the two others may be explained by noting the fact that the HOMO in the AlNNT is mainly localized on the N atoms while the LUMO is located on the Al ones, resulting in more strong HOMO/LUMO interaction. As a result, the transferred charge (0.188 *e*) from the HCN molecule to the tube in configuration **B** is remarkably more than that of the configuration **A** (0.002 *e*). The obtained results indicate that the HCN molecule undergoes a weak physical adsorption on the pristine AlNNTs due to weak van der Waals interaction between the AlNNT and HCN. From Table 1, no distinct changes can be concluded in the E_g values, indicating that the adsorption almost does not significantly influence the electric properties of the pristine AlNNT.

Thus, we conjecture that the pristine AlNNT is insensitive toward the HCN molecule, regardless of the adsorption sites of Al or N, suggesting that the pristine AlNNT may be not suitable for detecting the presence of HCN. It is noteworthy to say that although the change of E_g in configuration **B** has not shown definite trend (as shown in Fig. 2b), the DOS near the HOMO and LUMO levels has a change compared to that of the pristine tube, which would result in a

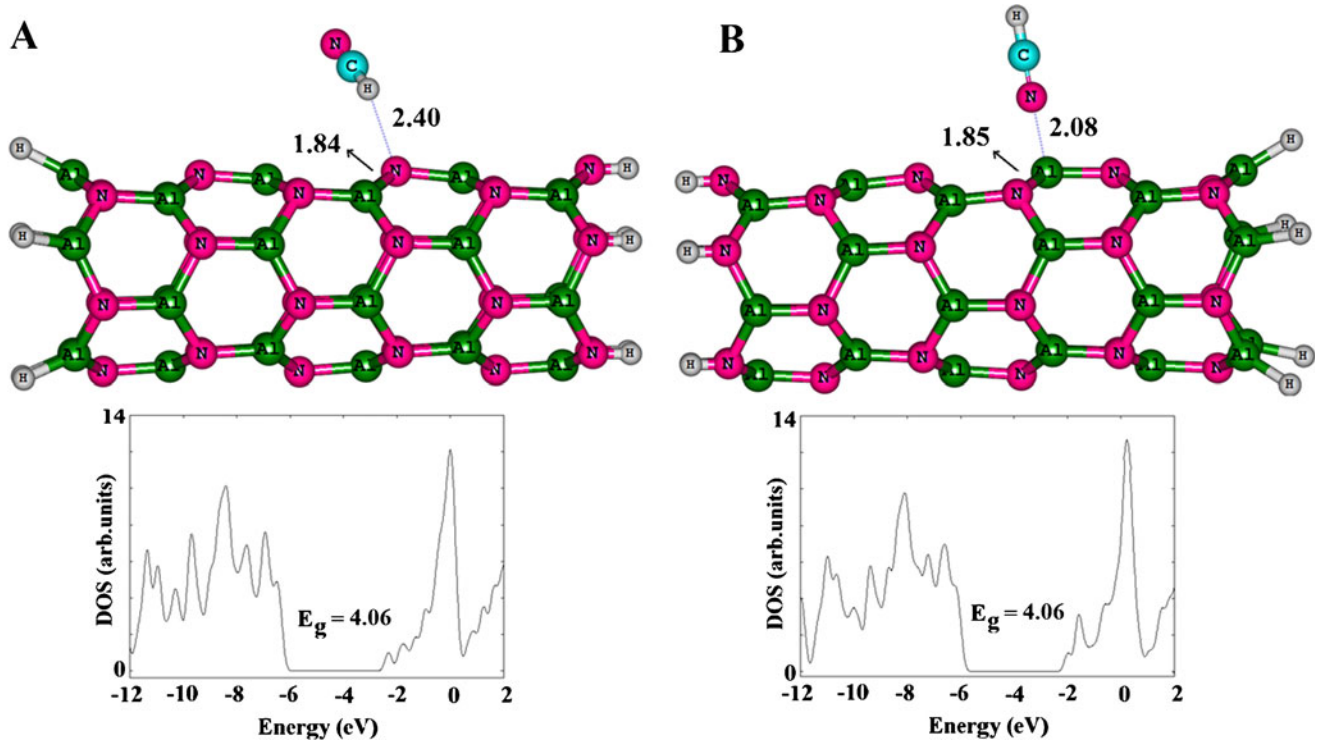

Fig. 2 Models for two stable adsorption states for a HCN molecule on the pristine AlNNT and corresponding density of states (DOS) plots. Distances are in Å

Fermi level enhancement from −4.26 to −4.01 eV due to charge transfer to the AlNNT.

HCN adsorption on the Al-rich AlNNT

In the next step, we have studied the interaction of defected AlNNT with a HCN molecule. Among various native defects, we have focused on aluminum antisite (Al_N), in which an aluminum atom sits at the original nitrogen site while being surrounded by three aluminum atoms, as shown in Fig. 3. Substituting the N atom by the impurity of Al (antisite defect), geometric structure of the AlNNT is dramatically distorted. In the optimized Al-rich AlNNT, the mentioned impurity atom is projected out of the tube surface to reduce the stress of being larger in size, compared to the N atom. The calculated bond lengths are 2.48 and 2.55 Å for the Al–Al bonds in the defected tube, being much longer than the corresponding Al-N bonds in the pristine tube. Also, the Al–Al–Al angles in defected AlNNT are 103° and 88° which are smaller than the Al-N-Al angles in the pristine tube (116° and 110°). Based on the obtained results from natural bond orbital (NBO) analysis, it can be attributed to the change of defect site hybridization from sp^2 to nearly sp^3.

Subsequently, we have explored HCN adsorption on the Al-rich tube by locating the molecule above the impurity atom with different initial orientations including H, C, or N atom of the molecule being close to the Al atom. The double-acceptor antisite can interact strongly with the HCN molecule in such a way that results in C≡N bond cleavage. This type of interaction is analogous to the dihydrogen interaction in boron-doped carbon nanostructures [40], where a closed-shell H_2 is attracted by a single acceptor state of the carbon-substituted boron. We have identified four distinct adsorptive stable configurations of the HCN/tube, as shown in Fig. 4. In all possible configurations, C≡N bond of the molecule located atop the parallel (configurations **P** and **Q**) and diagonal (configurations **R** and **S**) Al_N-Al bond of the defected tube. The major difference between the four configurations is the orientation of the C and N atoms of the HCN.

As shown in Table 2, the E_{ad} values corresponding to various adsorption configurations are in the range of −1.75 to −2.21 eV. The configuration **S** gives rise to an E_{ad} of −2.21 eV, which is higher than the E_{ad} values for the **P** (−2.12 eV), **Q** (−1.75 eV), and **R** (−1.78 eV). Calculated molecular electrostatic surface (Fig. 5) of the HCN shows that less negative E_{ad} value of the HCN from its N head to the Al_N atom is attributed to the partial negative charge on the N atom which makes it motionless toward the partially negative sites of Al_N atoms of the nanotube. Based on Mulliken charge analysis, Al_N atom has partial negative charge in the defected tube (unlike three neighboring Al atoms), so that a charge transfer (0.313 *e*) from the tube to the HCN is predicted.

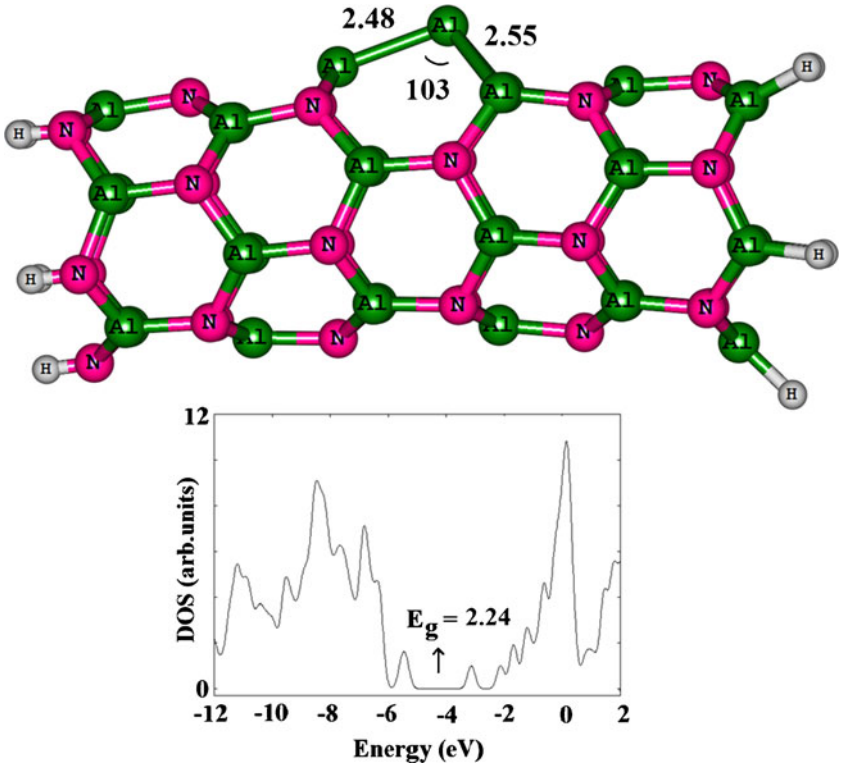

Fig. 3 Partial structure of Al-rich AlNNT and its density of states (DOS) (bonds in Å)

In the most stable configuration (**S**, Fig. 4), C≡N bond of the HCN molecule lies on diagonal Al_N–Al bond of the AlNNT, in which C and N atoms of the molecule are located atop the antisite Al atoms of the AlNNT with bond lengths of 1.96 Å (Al_N–N) and 1.26 Å (Al–C), respectively. In this configuration, the adsorption induces an apparent local structural deformation to both the HCN molecule and the AlNNT. In this configuration, the length of Al_N–Al bond attached to HCN is increased from 2.48 to 3.17 Å, and also the HCN molecule undergoes a structural distortion to a bent geometry and triple-bond breaking of the C≡N bond. The H-C-N bond angle is 122º, and the broken C≡N bond is significantly elongated from 1.15 Å in the free HCN to 1.26 Å on top of the Al_N. Calculated vibrational frequency

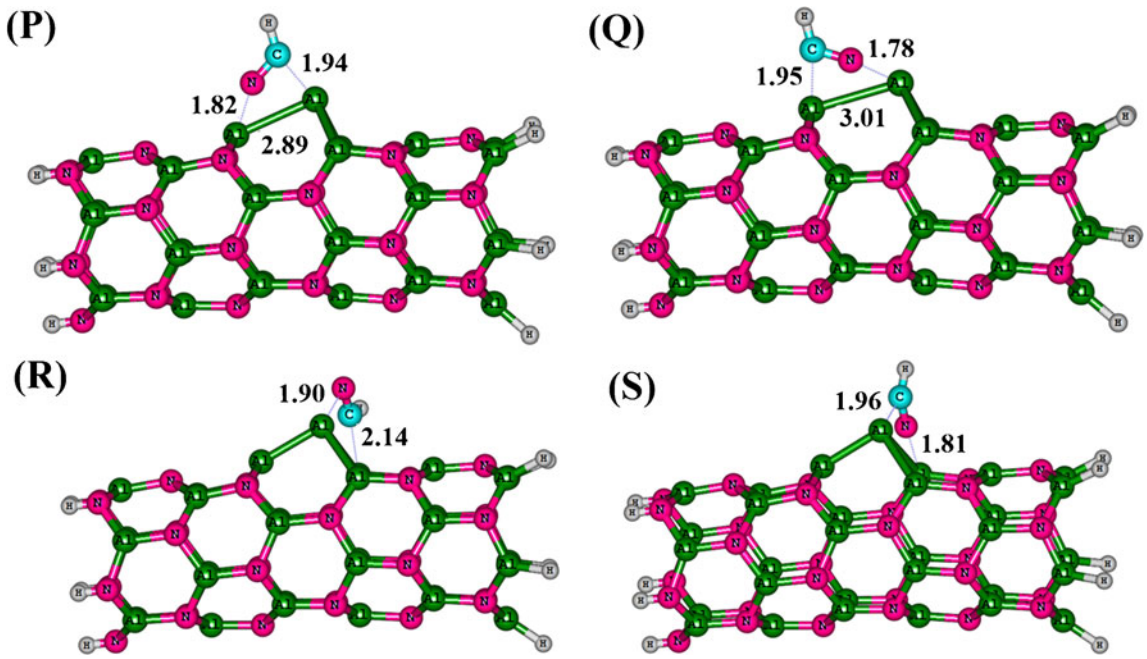

Fig. 4 Models for four stable adsorption states for a HCN molecule on the Al-rich AlNNT. Distances are in Å

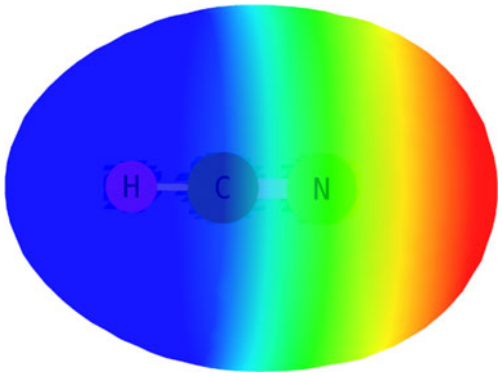

Fig. 5 Computed electrostatic potentials on the molecular surfaces of a single HCN molecule. Color ranges, in a.u.: *blue*, more positive than 0.010; *green*, between 0.010 and 0; *yellow*, between 0 and −0.015; *red*, more negative than −0.015

of the C≡N in the configuration **S** is about 1414 cm^{-1} which is smaller than that in the configuration **B** (2098 cm^{-1}), confirming much stronger adsorption of HCN on the Al-rich AlNNT in comparison with the pristine tube.

For the second most stable configuration (**P**, Fig. 4), C≡N bond of the HCN molecule lies on the parallel Al_N–Al bond of defected AlNNT with corresponding bond lengths of 1.82 and 1.94 Å. It can be seen that the C and N atoms of the HCN molecule are bonded to the Al_N and Al atoms of the AlNNT in both the most and the second most stable configurations. A question that immediately arises is why the diagonal bond (**S** configuration) is more favorable than the parallel bond (**R** configuration) for HCN adsorption. As AlNNTs are obtained by rolling the AlN sheets, the diagonal bonds have a larger local curvature in zigzag AlNNTs and are more reactive than the bonds in parallel to the tube axis.

In Table 2, we have summarized the obtained results for E_{ad}, Q_T, and E_g for HCN adsorption on the Al-rich AlNNT. Calculated DOS of defected AlNNT is shown in Fig. 3, indicating that its E_g value is reduced to 2.24 eV compared to the pristine AlNNT. The DOS plot shows clearly that the Al-rich AlNNT is still a wide-gap semiconductor with a defect-related gap state. The local DOS plot confirms that the AlN defect introduces the unoccupied double-acceptor defect state in the middle of the energy gap, and also occupies defect states near the valence band edge. DOS plots of the HCN/Al-rich AlNNT for all configurations show a considerable change, indicating that the electronic properties of the defected AlNNT are very sensitive toward the toxic HCN adsorption. It is revealed from DOS plots that the valence levels in all of the complexes are approximately similar to that of the defected tube, while the conduction levels significantly shift downward.

As seen in Fig. 6, the largest change in electronic properties is observed in more stable configurations, so that the E_g value of the Al-rich AlNNT is dramatically increased from 2.24 eV to 2.88–3.03 eV (by about 28.5–35.2 % change) in the adsorbed form, which would result in an

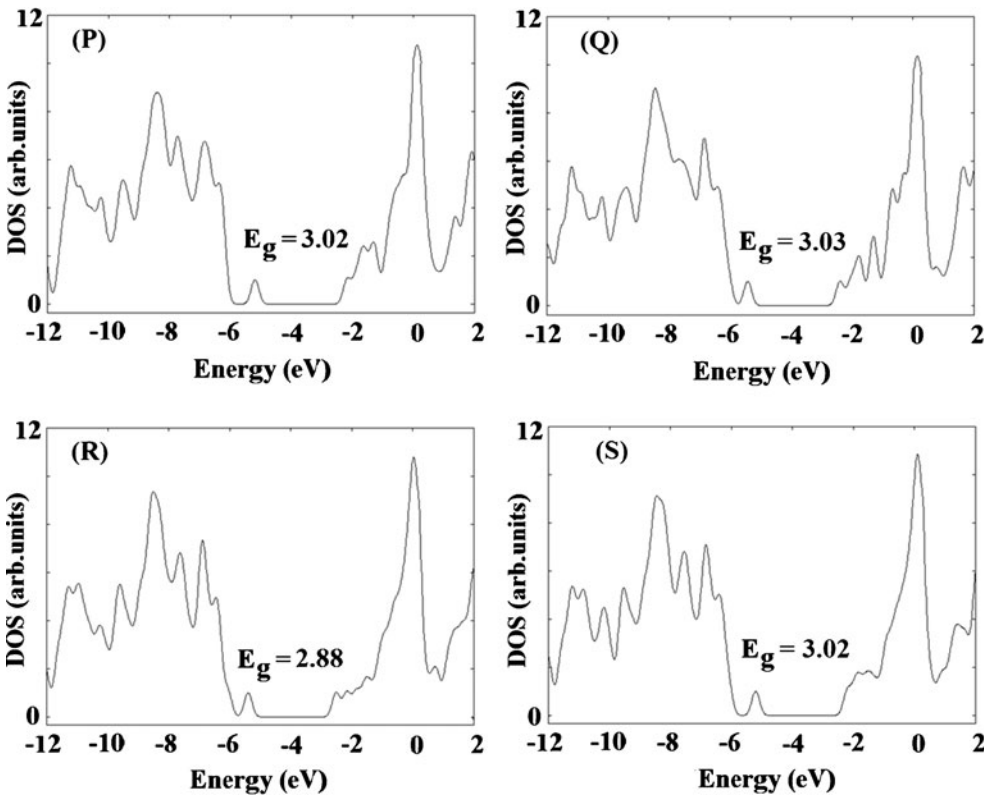

Fig. 6 DOS plots for HCN-adsorbed Al-rich AlNNT

electrical conductivity change in the defected tube according to the following equation:

$$\sigma \propto \exp\left(\frac{-E_g}{2kT}\right), \quad (2)$$

where σ is the electric conductivity, and k is the Boltzmann constant [41]. According to the equation, larger values of E_g at a given temperature lead to smaller electric conductivity. Therefore, the observed substantial increment of E_g in Al-rich AlNNT upon the adsorption process induces a change in the electrical conductance of the defected tube. According to the obtained results, it can be seen that Al-rich AlNNTs can effectively interact with toxic HCN molecule, and their electronic and transport properties are dramatically changed upon exposure to this molecule. So we believe that making Al-rich defects may be a good strategy for improving the sensitivity of AlNNTs toward HCN, which cannot be trapped and detected by the pristine AlNNT.

Conclusion

Geometric structures and electronic properties of the pristine and Al-rich AlNNTs in the presence and absence of an adsorbed HCN molecule were explored using density functional theory. It was found that the HCN molecule interacts with the pristine AlNNT via van der Waals forces, but it presents much higher reactivity toward the antisite defected-AlNNT. Adsorption energy changes corresponding to the adsorption of HCN on the pristine and defected AlNNTs were calculated to be in the range of −0.16 to −0.62 eV and −1.75 to −2.21 eV, respectively. Based on the analysis of density of states, it was suggested that Al-rich AlNNTs may be used in a gas sensor to detect and monitor the HCN molecule. Mechanism of detection is based on the change in conductance of the Al-rich AlNNTs upon the adsorption process, which provides a measurable electrical signal.

References

1. Wang R, Zhang D, Zhang Y, Liu C (2006) J Phys Chem B 110:18267–18271
2. Wang X, Liew KM (2011) J Phys Chem C 115:10388–10393
3. Field CR, Yeom J, Salehi-Khojin A, Masel RI (2010) Sensor Actua B-Chem 148:315–322
4. Govind N, Andzelm J, Maiti A (2008) IEEE Sensors J 8:837–841
5. Kong J, Franklin NR, Zhou C, Chapline MG, Peng S, Cho K, Dai H (2000) Science 287:622–625
6. Collins PG, Bradley K, Ishigami M, Zettl A (2000) Science 287:1801–1804
7. Dinadayalane TC, Kaczmarek A, Lukaszewicz J, Leszczynski J (2007) J Phys Chem C 111:7376–7383
8. Beheshtian J, Ahmadi Peyghan A, Bagheri Z (2012) Phys E 44:1963–1968
9. Ahmadi A, Hadipour NL, Kamfiroozi M, Bagheri Z (2012) Sens Actuators B: Chem 161:1025–1029
10. Ahmadi Peyghan A, Omidvar A, Hadipour NL, Bagheri Z, Kamfiroozi M (2012) Phys E 44:1357–1360
11. Beheshtian J, Baei MT, Peyghan AA, Bagheri Z (2012) J Mol Model 18:4745–4750
12. Beheshtian J, Kamfiroozi M, Bagheri Z, Ahmadi A (2011) Physica E 44:546–549
13. Beheshtian J, Peyghan AA, Bagheri Z (2012) Sens Actuators B: Chem 171–172:846–852
14. Dinadayalene TC, Murray JS, Concha MC, Politzer P, Leszczynski J (2010) J Chem Theor Comp 6:1351–1357
15. Saikia N, Deka RC (2012) J Mol Model. doi:10.1007/s00894-012-1534-9
16. Xie Y, Hou YP, Zhang JM (2012) Appl Surf Sci 258:6391–6398
17. Ahmadi A, Beheshtian J, Kamifiroozi M (2012) J Mol Model 18:1729–1734
18. Gao G, Park SH, Kang HS (2009) Chem Phys 355:50–54
19. An W, Wu X, Zeng XC (2008) J Phys Chem C 112:5747–5755
20. Lin F, Zhou G, Li Z, Li J, Wu J, Duan W (2009) Chem Phys Lett 475:82–85
21. Choi H, Park YC, Kim YH, Lee YS (2011) J Am Chem Soc 133:2084–2087
22. Hamadanian M, Khoshnevis B, Kalantari Fotooh G (2011) Struct Chem 22:1205–1211
23. Beheshtian J, Baei MT, Peyghan AA, Bagheri Z (2012) J Mol Model. doi:10.1007/s00894-012-1476-2
24. Stan G, Ciobanu C, Thayer T, Wang G, Creighton J, Purushotham K, Bendersky L, Cook R (2009) Nanotechnology 20:35706–357014
25. Zhang D, Zhang R (2003) Chem Phys Lett 371:426–432
26. Tondare V, Balasubramanian C, Shende S, Joag D, Godbole V, Bhoraskar S, Bhadhade M (2002) Appl Phys Lett 80:4813–4815
27. Balasubramanian C, Bellucci S, Castrucci P, Crescenzi M, Bhoraskar S (2004) Chem Phys Lett 383:188–191
28. Yin B, Bando Y, Zhu Y, Li M, Tang C, Golberg D (2005) Adv Mater 17:213–217
29. Contreras ML, Avila D, Alvarez J, Rozas R (2010) Struct Chem 21:573–581
30. Peralta-Inga Z, Lane P, Murray J, Boyd S, Grice M, O'Connor C, Politzer P (2003) Nano Lett 3:21–28
31. Wang R, Zhang D, Liu Y, Liu C (2009) Nanotechnology 20:505704(1)–505704(8)
32. Parr RG, Yang W (1989) Density-functional theory of atoms and molecules. Oxford University Press, New York
33. Schmidt M et al (1993) J Comput Chem 14:1347–1363
34. Beheshtian J, Soleymanabadi H, Kamfiroozi M, Ahmadi A (2012) J Mol Model 18:2343–2348
35. Beheshtian J, Bagheri Z, Kamfiroozi M, Ahmadi A (2012) J Mol Model 18:2653–2658
36. Beheshtian J, Bagheri Z, Kamfiroozi M, Ahmadi A (2012) Struct Chem 23:653–657
37. Tomić S, Montanari B, Harrison NM (2008) Phys E 40:2125–2127
38. Lee C, Yang W, Parr RG (1988) Phys Rev B 37:785–789
39. O'Boyle NM, Tenderholt AL, Langner KM (2008) J Comp Chem 29:839–845
40. Kim YH, Zhao Y, Williamson A, Heben MJ, Zhang SB (2006) Phys Rev Lett 96:016102(1)–016102(4)
41. Li S (2006) Semiconductor physical electronics, 2nd edn. Springer, Heidelberg